Supporting Information

Rapid and Highly Sensitive Immunosorbent Assay to Monitor Helicases Unwinding Diverse Nucleic Acid Structures

Jia-En Wang,[†a] Ying-Chen Zhou,[†a] Bi-Han Wu,[a] Xiu-Cai Chen,[a] Junqiu Zhai,[b] Jia-Heng Tan,[a] Zhi-Shu Huang[a] and Shuo-Bin Chen,[a,*]

[a]*School of Pharmaceutical Sciences, Guangdong Provincial Key Laboratory of New Drug Design and Evaluation, Sun Yat-sen University, Guangzhou 510006, China*

[b]*Guangzhou University of Chinese Medicine, Guangzhou, Guangzhou 510330, China*

[*]To whom correspondence should be addressed. *(S.-B. Chen) E-mail: chenshb8@mail.sysu.edu.cn.

[†]These authors contributed equally to this work.

Table of Contents

Table S1. Oligonucleotide sequences used in the study. The hybrid sequences are colored in red. The G4 and hairpin forming sequences are colored in blue.

Name	Strand	Sequence (5'-3')
Fork1	A	Biotin-TTTTTTTTTTCGTACCCGATGTGTTCGTTC
	B	DIG-GAACGAACACATCGGGTACGTTTTTTTTTT
Fork2	A	Biotin-TTTTTTTTTTCGTACCCGATGTGTTCGTTC
	B	DIG-GAACGAACACATCGGGTACG
Fork3	A	Biotin-TTTTTTTTTTCGTCGAGCAGAG
	B	DIG-CTCTGCTCGACGTTTTTTTTTT
Fork4	A	Biotin-TTTTTTTTTTCGTACCCGATGTGTTCGTTCAACTTAGC
	B	DIG-GCTAAGTTGAACGAACACATCGGGTACGTTTTTTTTTT
Bub1	A	Biotin-TTTTTTTTTTCTGCTAATGTAATTTTTTTTTTTTTACGACAAGATCTTTTTTTTTT
	B	DIG-GATCTTGTCGTACAGGATCGTTACATTAGCAG
Bub2	A	Biotin-TTTTTTTTTTCTGCTAATGTAATTTTTTTTTTTTTACGACAAGATC
	B	DIG-GATCTTGTCGTACAGGATCGTTACATTAGCAG
HJ1	A	Biotin-TTTTTTTTTTCACCCGTTTCTACAGGATCGTTCGGTCTTAAG
	B	DIG-GATCTTGTCGTACAGGATCGTTACATTAGCAG
	C	CTTAAGACCGAACGATCCTGTACGACAAGATCTTTTTTTTTT
	D	CTGCTAATGTAACGATCCTGTAGAAACGGGTGTTTTTTTTTT
HJ2	A	Biotin-TTTTTTTTTTCACCCGTTTCTACAGGATCGTTCGGTCTTAAG
	B	DIG-GATCTTGTCGTACAGGATCGTTACATTAGCAG
	C	CTTAAGACCGAACGATCCTGTACGACAAGATC
	D	CTGCTAATGTAACGATCCTGTAGAAACGGGTG
DS1	A	Biotin-TTTTTTTTTTCGTCGAGCAGAGATGAGTTAGAGTTAGAGTTAGAGTTTTTTTTTT
	B	CTCTGCTCGACG-DIG
DS2	A	Biotin-TTTTTTTTTTCGTCGAGCAGAGATTTTTTTTTTT
	B	CTCTGCTCGACG-DIG
GQ1	A	Biotin-TTTTTTTTTTCGTCGAGCAGAGATGGGTTTGGGTTTGGGTTTGGGTTTTTTTTTT
	B	CTCTGCTCGACG-DIG
GQ2	A	Biotin-TTTTTTTTTTCGTCGAGCAGAGATGGGTTAGGGTTAGGGTTAGGGTTTTTTTTTT
	B	CTCTGCTCGACG-DIG
GQ3	A	Biotin-TTTTTTTTTTCGTCGAGCAGAGATTGGGTTTGGGTGGGTTTGGGTTTTTTTTTT
	B	CTCTGCTCGACG-DIG
GQ4	A	Biotin-TTTTTTTTTTCGTCGAGCAGAGATGGGGTTTGGGGTTTGGGGTTTGGGGTTTTTTTTT
	B	CTCTGCTCGACG-DIG
HP1	A	Biotin-TTTTTTTTTTCGTCGAGCAGAGATCGGTACTTTTGTACCGATTTTTTTTTTT
	B	CTCTGCTCGACG-DIG
HP2	A	Biotin-TTTTTTTTTTCGTCGAGCAGAGCGCGCGCGTTTTCGCGCGCGTTTTTTTTTT
	B	CTCTGCTCGACG-DIG
HP3	A	Biotin-TTTTTTTTTTCGTCGAGCAGAGATATATATTTTTATATATATTTTTTTTTT
	B	CTCTGCTCGACG-DIG

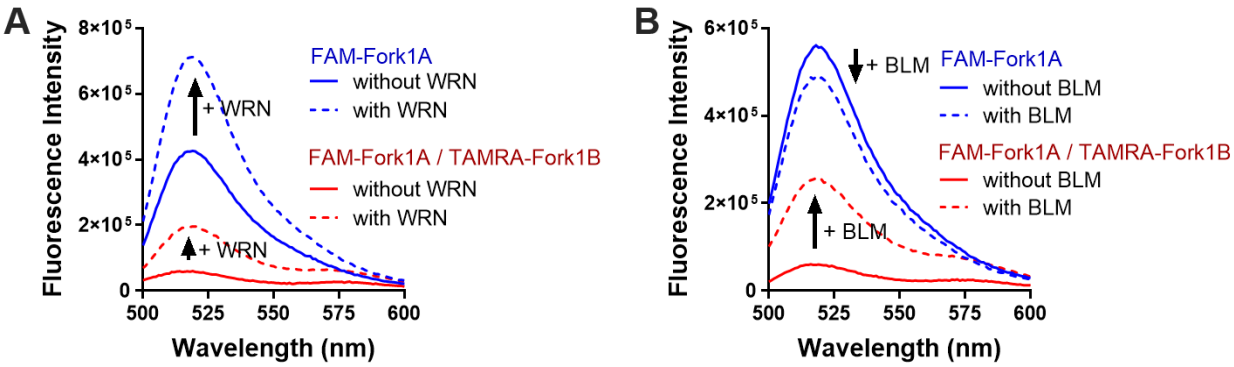

Figure S1. Fluorescence spectra of fluorescent DNA with 100 nM WRN (A) and BLM (B).

The FAM labelled Fork1A (FAM-Fork1A) was heated to 95°C for 10 min, then slowly annealed to room temperature with or without the TAMRA labelled Fork1B (TAMRA-Fork1B) in Tris buffer (30 mM NaCl, 10 mM Tris-HCl, pH 7.4), respectively. The fluorescence spectra of DNA (20 nM) were collected upon excitation wavelength at 480 nm. In the FRET assay, the FAM-Fork1A and TAMRA-Fork1B will quench when hybrid. The unwinding activity could be determined by the increased fluorescence as the hybrid sequences separated. However, the fluorescence intensity of both single-strand DNA (FAM-Fork1A) and duplex DNA (FAM-Fork1A with TAMRA-Fork1B) were changed after adding BLM and WRN proteins in the absence of ATP. Because WRN and BLM unwind duplex DNA in an ATP-dependent manner, the change in fluorescence came from the unexpected influence of the helicase on the fluorophores. The influence on fluorophores will possibly interfere with the unwinding detection.

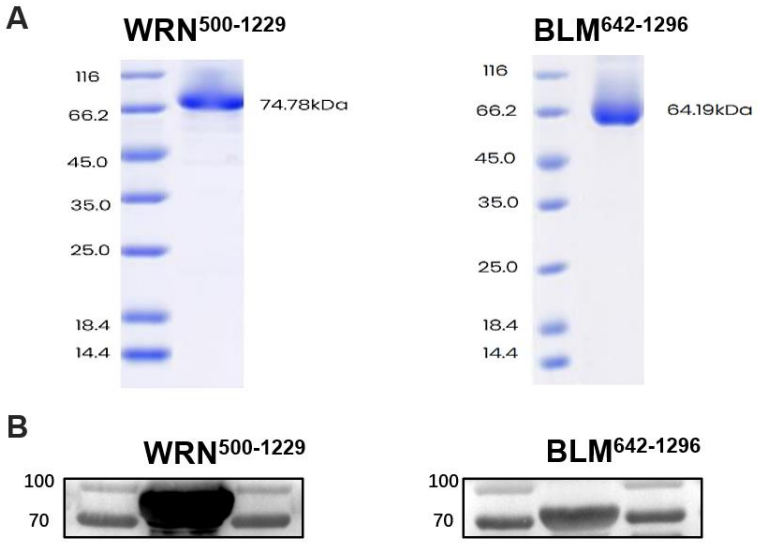

Figure S2. Purity Characterization of WRN and BLM by SDS-PAGE (A) and Western Blot (B).

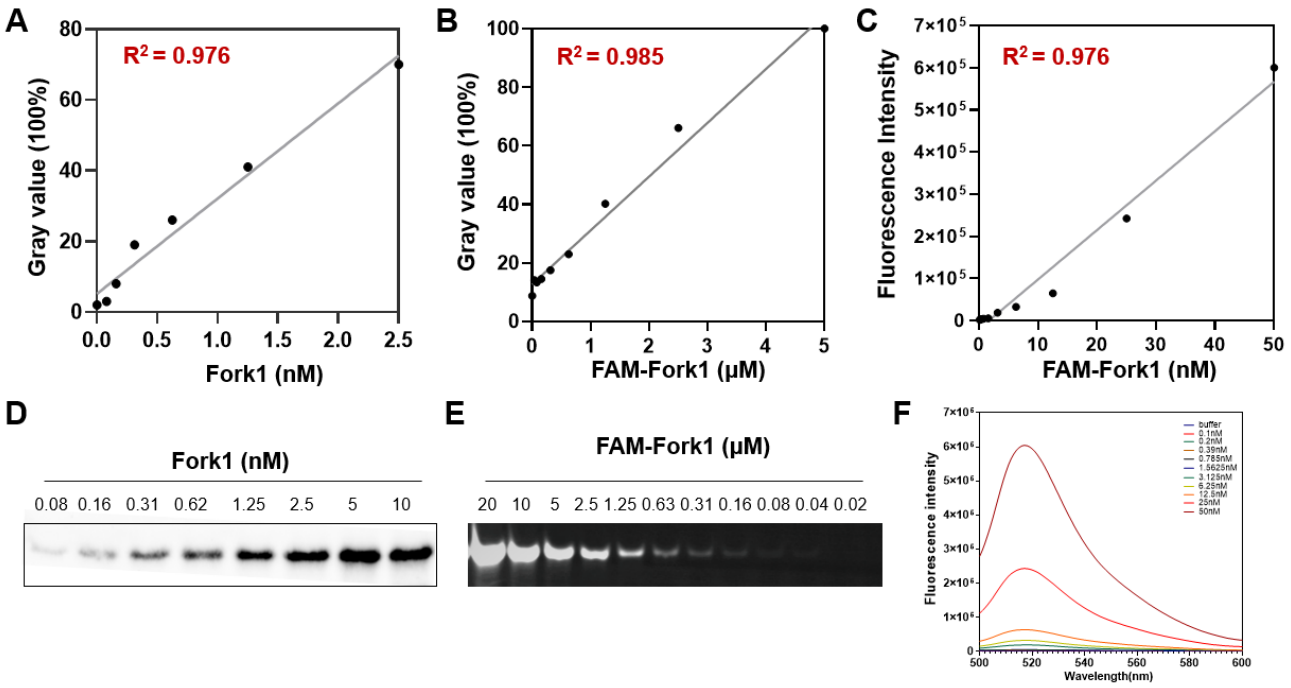

Figure S3. Standard curves, depicting the linear range fitting of Fork1 in the chemiluminescent EMSA (A), fluorescent EMSA (B) and fluorescence spectra (C). In the fluorescence methods, FAM was labelled on the A-strand of Fork1 substrate (FAM-Fork1). In the chemiluminescent EMSA, the biotin labelled Fork1 was transferred to the member and recognized by the HRP-linked streptavidin. The EMSA and spetra data was shown in D-F, below their curve.

Table S2. Linear range and LOD of Fork1 in the different methods.

Methods	Instrument	Linear range (nM)	LOD (nM)
Immunosorbent Assay	Well-plate reader	0-2.5	0.12
Chemiluminiscent EMSA	Gel imager	0-2.5	0.16
Fluorescent EMSA	Gel imager	0-5000	1700
Fluorescence Spectra	Spectrophotometer	0-50	2.86

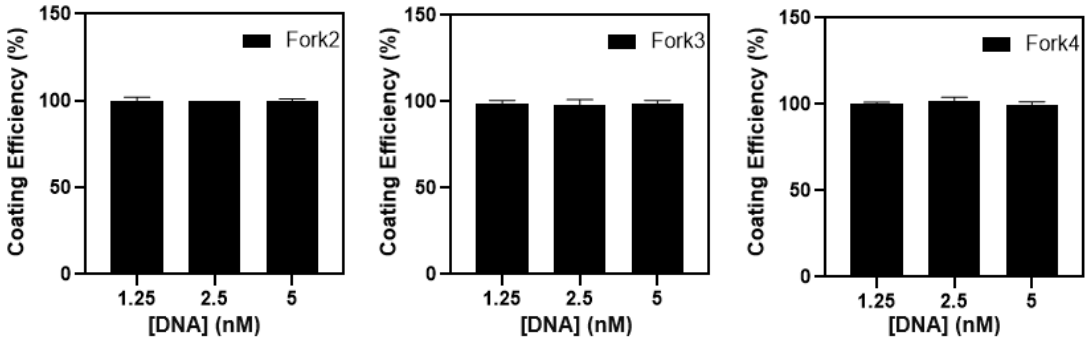

Figure S4. Coating efficiency of the forked substrates in the immunosorbent assay.

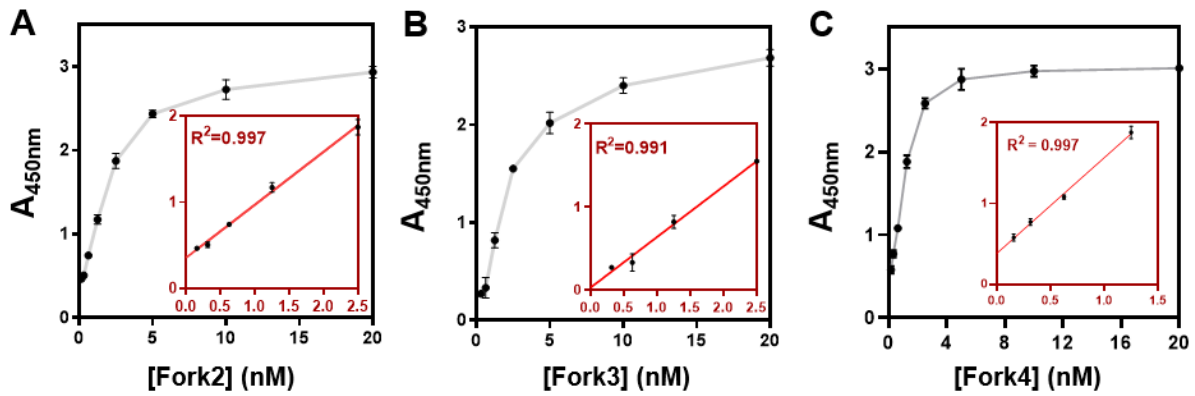

Figure S5. Detection of the forked DNAs by the immunosorbent assay. The standard curve, depicting the linear range fitting, is shown in the inset with the x-axis and y-axis using the same unit of measurement.

Table S3. Linear range and LOD of the forked DNA substrates in the immunosorbent assay.

DNA substrate	Linear range (nM)	LOD (nM)
Fork1	0-2.5	0.12
Fork2	0-2.5	0.10
Fork3	0-2.5	0.18
Fork4	0-1.25	0.02

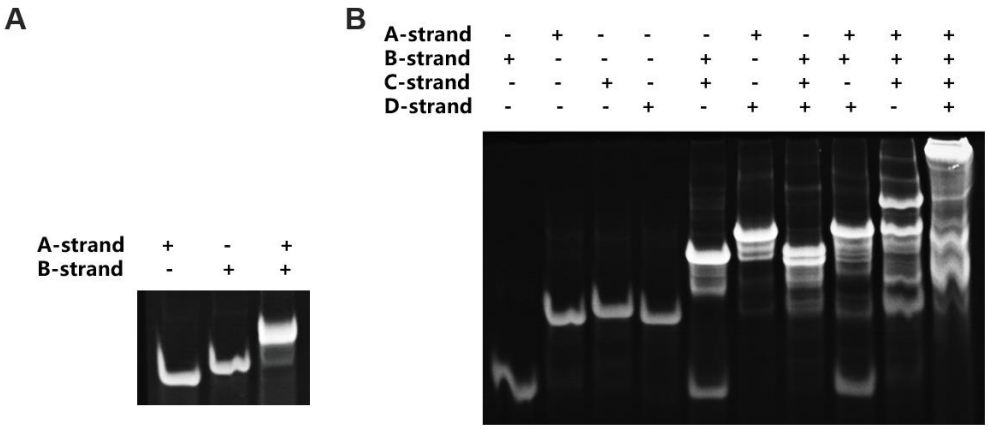

Figure S6. Verification of bubble (A) and HJ (B) formations by EMSA.

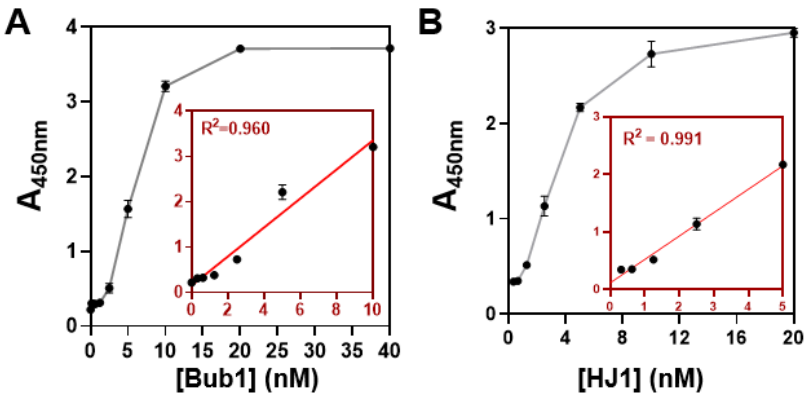

Figure S7. Detection of the bubble (A) and HJ (B) substrates by the immunosorbent assay. The standard curve, depicting the linear range fitting, is shown in the inset with the x-axis and y-axis using the same unit of measurement.

Table S4. Linear range and LOD of the bubble and HJ substrates in the immunosorbent assay.

DNA substrate	Linear range (nM)	LOD (nM)
Bub1	0-10	0.63
HJ1	0-10	0.71

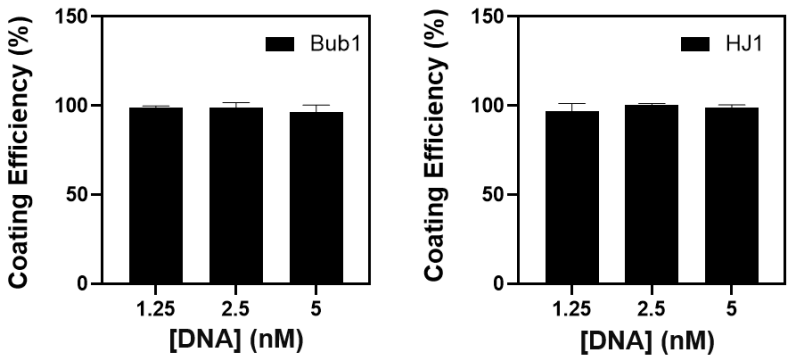

Figure S8. Coating efficiency of the bubble and HJ substrates in the immunosorbent assay.

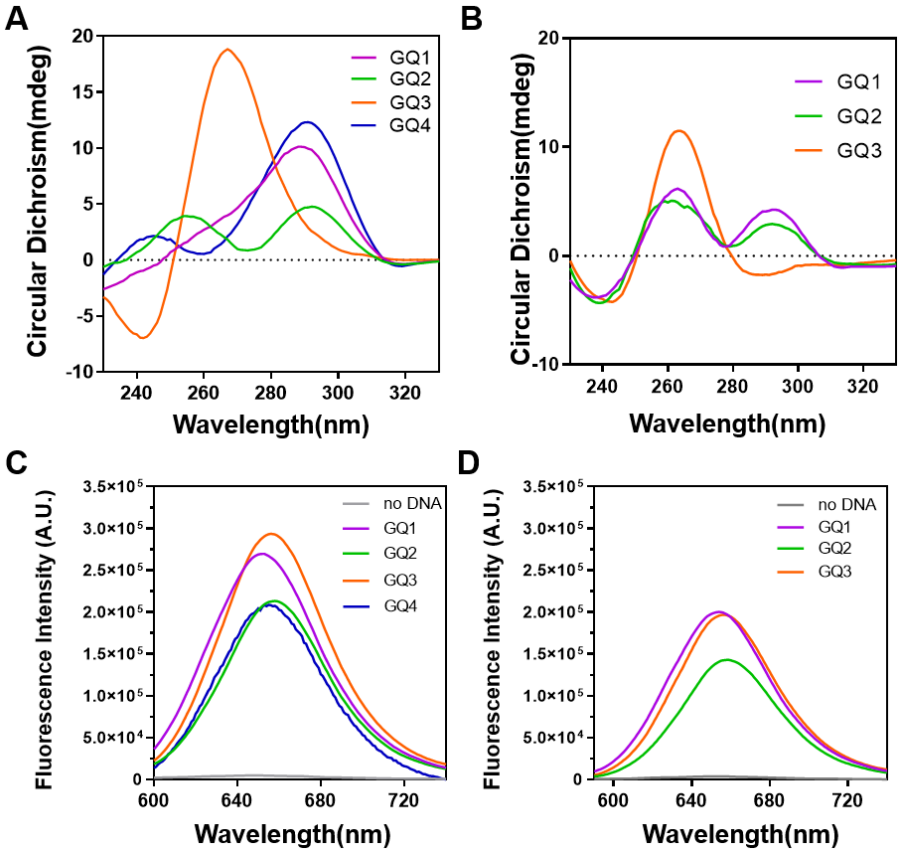

Figure S9. Validation of the G4 formations. CD spectra of G4 substrates (2 μM) with 100 mM KCl (A) or without KCl (B). Fluorescence spectra of G4 substrates (2 μM) with 100 mM KCl (C) or without KCl (D) in the presence of G4 light-up probe **ISCH-1** (1 μM).

To determine the G4 formation, the CD signal for the duplex region was deducted by the CD spectra of DS2. On the one hand, with KCl, all the G4 substrates showed a positive peak at around 260 nm or 290 nm in the CD spectra and strong fluorescence in the fluorescence spectra, suggesting stable formation of G4. On the other hand, without KCl, all the G4 substrates showed much weaker peaks in the CD spectra and weaker fluorescence in the fluorescence spectra, suggesting unstable or partly formation of G4.

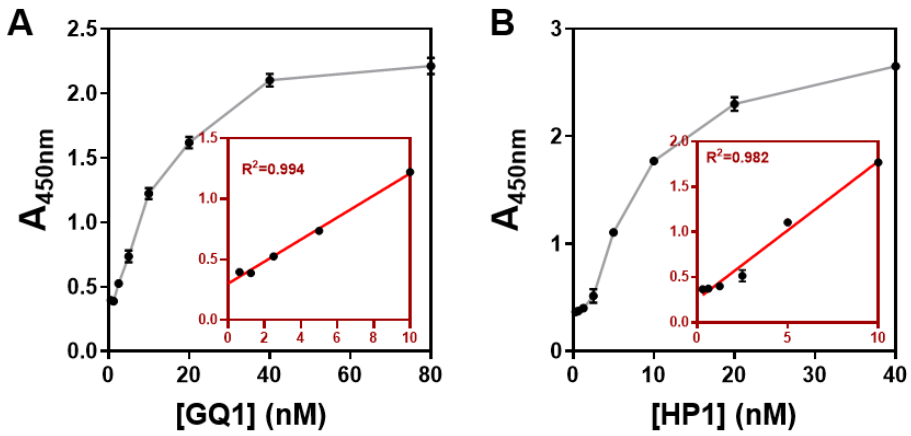

Figure S10. Detection of the G4 (A) and hairpin (B) substrates by the immunosorbent assay. The standard curve, depicting the linear range fitting, is shown in the inset with the x-axis and y-axis using the same unit of measurement.

Table S5. Linear range and LOD of the G4 (A) and hairpin (B) substrates in the immunosorbent assay.

DNA substrates	Linear range (nM)	LOD(nM)
GQ1	0-10	1.12
HP1	0-10	0.71

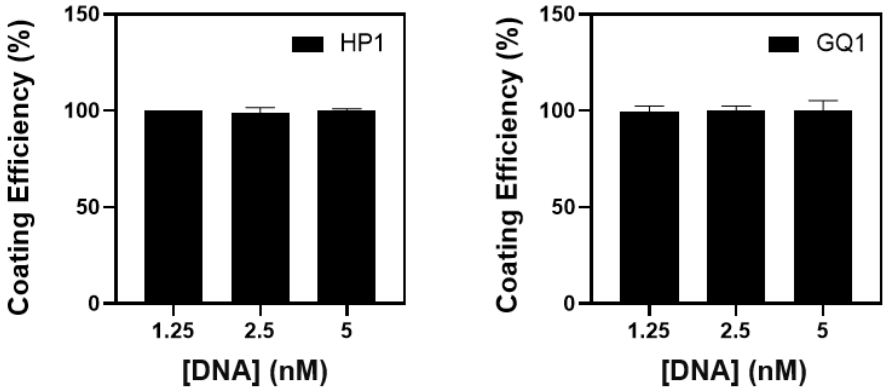

Figure S11. Coating efficiency of the G4 and hairpin substrates in the immunosorbent assay.

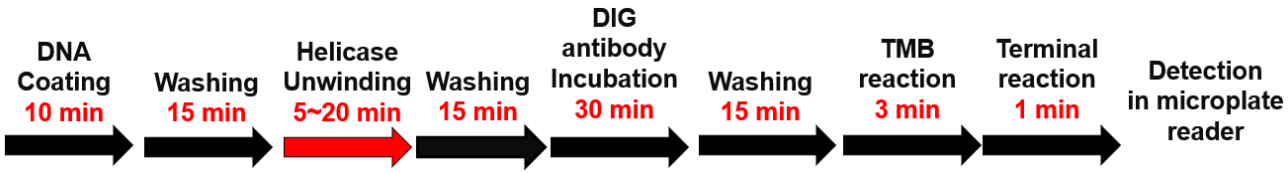

Figure S12. The procedure of the immunosorbent helicase unwinding assay.

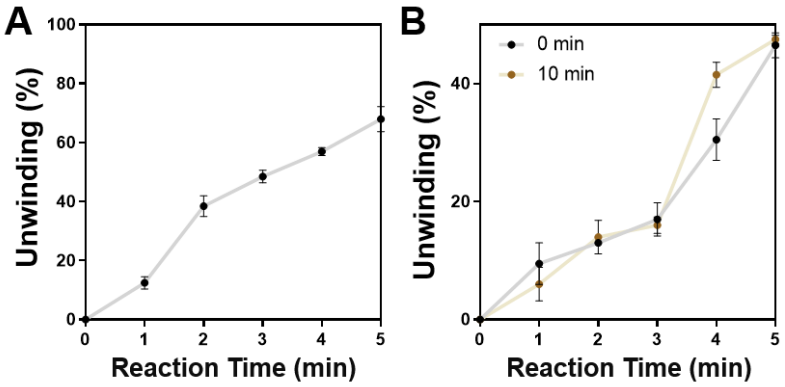

Figure S13. the ATP hydrolysis activity (B) in WRN unwinding Fork1 was detected in parallel with the immunosorbent helicase unwinding assay (A). The reaction mixture was collected after the Helicase Unwinding Step (Figure S12), and the ATP hydrolysis of the collection was determined immediately (0 min) or after 10 min stored at 37 ℃. Notably, the ATP hydrolysis in the collection was not changed even stored at 37 ℃ for 10 min. The above result suggests the ATP hydrolysis in the reaction mixture was terminated when removed from the well-plate. It is reasonable that the DNA was separated from the helicase, and the DNA-dependent ATPase activity of RecQ helicase was terminated. These characteristics might enable the coupling detection of unwinding and ATPase activity more accurately.